

(d, Li^6) Reactions in Light Elements and Distorted-Wave Born Approximation Calculations*

L. J. DENES,[†] W. W. DAHNICK, AND R. M. DRISKO[‡]

University of Pittsburgh, Pittsburgh, Pennsylvania

(Received 17 March 1966)

Differential cross sections for (d, Li^6) reactions have been measured for C^{13} , O^{17} , O^{18} , and F^{19} targets in addition to those reported previously for C^{12} , O^{16} , and F^{19} . Li^6 particles were identified by using time-of-flight analysis in conjunction with energy analysis. (d, Li^6) reactions for all six targets, investigated at incident deuteron energies near 15 MeV, have large total cross sections (4.2 to 0.6 mb). The angular distributions are diffraction-like, and show forward peaking and minor sensitivity to energy changes of a few hundred keV. A theoretical interpretation of the (d, Li^6) reactions is given in terms of a simple direct four-nucleon transfer mechanism. Most calculations are made in the zero-range distorted-wave Born approximation (DWBA). The reaction form factor is calculated in the alpha transfer limit; i.e., an α -cluster (with predictable quantum numbers) is assumed to exist in the target at the instant of the reaction and to be transferred as a whole. The cluster wave function is generated in a Saxon well of a depth determined by the α separation energy. Best-fit optical-model parameters for 15-MeV deuterons were used to generate the incident deuteron waves. All Li^6 distorted waves were based on an optical-model fit to the $\text{C}^{12}(\text{Li}^7, \text{Li}^7)\text{C}^{12}$ scattering at 7 MeV. No adjustable parameters were used. In spite of these restrictions and the simplicity of the model, good agreement between data and calculations is observed for C^{12} , C^{13} , O^{16} , O^{17} , and O^{18} . Agreement for $\text{F}^{19}(\text{Li}^6)\text{N}^{15}$ could be obtained only by parameter adjustments. The normalization of the DWBA predictions also appears to be in general agreement with the absolute magnitude for these reactions, and tentative spectroscopic factors for the reactions are obtained.

A. INTRODUCTION

RECENTLY much of the work on light nuclei has been focused on the nature of many-nucleon correlations. There has been considerable interest in the question whether significant clustering of nucleons exists in nuclei, especially in the form of alpha-like clusters. It is well known that shell-model wave functions can be rewritten in cluster form,^{1,2} and more recent theoretical investigations³⁻⁸ have shown that even without residual interactions the independent-particle model predicts large 4 nucleon parentages if these nucleons are coupled to 0^+ . Several experimental approaches have been used to probe α -cluster phenomena in nuclei. These include high-energy "knock-

out" reactions of the type $(p, p\alpha)^{5,9-11}$ and $(\alpha, 2\alpha)^{10-14}$ as well as "pickup" reactions such as $(d, \text{Li}^6)^{15-23}$ and $(\alpha, \text{Be}^8)^{24}$. The present paper contains some new $d\text{-Li}^6$ data and a review of earlier work^{17,18} at 15 MeV.

In the past, stripping and pickup calculations have been very successful for investigating the single-particle aspect of nuclear structure, and it is natural to attempt to obtain corresponding information about correlated four-particle groups in the same theoretical framework. Since deuterons and Li^6 ions are strongly absorbed pro-

* Work done at the Sara Mellon Scaife Radiation Laboratory, and supported in part by the National Science Foundation.

[†] Present address: United Aircraft Research Laboratory, Hartford, Connecticut.

[‡] Permanent address: Oak Ridge National Laboratory, Oak Ridge, Tennessee.

¹ K. Wildermuth and T. Kananopolous, Nucl. Phys. **7**, 150 (1958); **9**, 449 (1958).

² G. C. Phillips and T. A. Tombrello, Nucl. Phys. **19**, 555 (1960), and references therein.

³ V. V. Balashov, V. G. Neudatchin, Yu. F. Smirnov, and N. P. Yudin, Zh. Eksperim. i Teor. Fiz. **37**, 1385 (1959) [English transl.: Soviet Phys.—JETP **10**, 983 (1960)].

⁴ S. Matthies, V. G. Neudatchin, and Yu. F. Smirnov, Nucl. Phys. **49**, 97 (1963).

⁵ V. V. Balashov, A. N. Boyarkina, and I. Rotter, Nucl. Phys. **59**, 417 (1964).

⁶ Yu. A. Kudejarov, S. Matthies, V. G. Neudatchin, and Yu. F. Smirnov, Nucl. Phys. **65**, 529 (1965).

⁷ V. V. Balashov and I. Rotter, Nucl. Phys. **61**, 138 (1965).

⁸ V. G. Neudatchin and Yu. F. Smirnov, Nucl. Phys. **66**, 26 (1965).

⁹ A. N. James and N. G. Pugh, Nucl. Phys. **42**, 441 (1963).

¹⁰ Y. Sakamoto, Nucl. Phys. **66**, 531 (1965).

¹¹ P. Beregi, N. S. Zelenskaja, V. N. Neudatchin, and Yu. F. Smirnov, Nucl. Phys. **66**, 513 (1965).

¹² G. Igo, L. F. Hansen, and T. J. Gooding, Phys. Rev. **131**, 337 (1963).

¹³ P. F. Donovan, J. V. Kane, Č. Zupančič, C. P. Baker, and J. F. Mollenauer, Phys. Rev. **135**, B61 (1964).

¹⁴ R. W. Bauer, G. Heymann, W. Kossler, N. S. Wall, and C. R. Gruhn, Rev. Mod. Phys. **37**, 369 (1965).

¹⁵ L. J. Denes, M. S. thesis, University of Pittsburgh, 1963 (unpublished); L. J. Denes and W. W. Daehnick, Bull. Am. Phys. Soc. **8**, 25 (1963).

¹⁶ D. S. Gemmel, J. R. Erskine, and J. P. Schiffer, Phys. Rev. **134**, B110 (1964).

¹⁷ W. W. Daehnick and L. J. Denes, Phys. Rev. **136**, B1325 (1964), and references therein.

¹⁸ L. J. Denes and W. W. Daehnick, Bull. Am. Phys. Soc. **10**, 120 (1965).

¹⁹ J. B. Gerhart, P. Mizera, and F. W. Slee, Cyclotron Research, University of Washington, 1964 (unpublished), p. 21; F. W. Slee, Bull. Am. Phys. Soc. **10**, 461 (1965).

²⁰ L. J. Denes, Ph. D. thesis, University of Pittsburgh, 1965 (unpublished).

²¹ D. Dehnhard, D. S. Gemmel, and Z. Vager, Bull. Am. Phys. Soc. **10**, 602 (1965).

²² R. S. Bender and E. Newman, Bull. Am. Phys. Soc. **10**, 602 (1965).

²³ W. W. Daehnick and L. J. Denes, Bull. Am. Phys. Soc. **11**, 30 (1966).

²⁴ R. E. Brown, J. S. Blair, D. Bodansky, N. Cue, and C. D. Kavaloski, Phys. Rev. **138**, B1394 (1965).

jectiles the (d, Li^6) reactions are surface reactions, which are favorable for our purpose, partly because they generally lead to characteristic diffraction-like angular distributions. As most evidence,^{2,25-27} such as the α - d separation energy of only 1.47 MeV supports a strong $d+\alpha$ parentage in Li^6 , the (d, Li^6) reaction seems suitable from the spectroscopic point of view.²⁸ Our analysis was undertaken with the hope that (d, Li^6) reactions can correctly be described in the framework of current direct-reaction theory (e.g., by the distorted-wave Born approximation, DWBA) as the transfer of an alpha cluster to a deuteron projectile.²⁹

B. DWBA CALCULATIONS FOR (d, Li^6) REACTIONS

DWBA cross sections were calculated using the code JULIE.³⁰ The reaction $A(d, \text{Li}^6)B$ is assumed to be of the type $(B+\alpha)(d, d+\alpha)B$. That is, the incident deuteron picks up an alpha cluster from the target nucleus A and only the component of the target wave function which has the form $A = B+\alpha$ is treated as relevant. The transition amplitude is then calculated in the zero range, distorted-wave Born approximation. However, three finite-range calculations were made using an exact finite range code³¹ and show no major qualitative change in angular distribution. The normalization change is small. As usual we assume that elastic scattering is the dominant process, and calculate the α pickup in first-order perturbation theory. And as usual, recoil and exchange terms are neglected. The neglect of such terms for targets as light as those in the present study may be serious.

The distorted waves are generated from the optical-model potentials which reproduce the observed elastic scattering from the targets or residual nuclei at the respective energies. The potentials used for both the incident and exit channels are of conventional form; the attractive real potential is of the Woods-Saxon volume form:

$$V(r) = -V \left[1 + \exp\left(\frac{r-r_0 A^{1/3}}{a}\right) \right]^{-1}.$$

The attractive imaginary potential is of a surface absorption form given as the derivative of a Woods-Saxon potential:

$$W(r) = +W' a' \frac{d}{dr} \left\{ \left[1 + \exp\left(\frac{r-r_0' A^{1/3}}{a'}\right) \right]^{-1} \right\}.$$

The Coulomb potential used is that of a uniform spherical charge distribution of radius $r_c A^{1/3}$.

The optical parameters used to obtain the distorted deuteron waves were obtained from optical-model fits to the elastic scattering of 15-MeV deuterons³² from the targets under investigation. These best-fit parameters are listed in Table I for each nucleus. Only one set of optical-model parameters was used to obtain distorted Li^6 waves for all the exit channels. These parameters are also given in Table I, and are based on a fit to Li^7 scattering from C^{12} at $E_{\text{lab}} = 7$ MeV.³³ This, unfortunately, was the extent of Li^6 or Li^7 elastic-scattering data available at the time of these calculations. Strictly speaking, our Li potential is only appropriate for the reaction $\text{O}^{17}(d, \text{Li}^7)\text{C}^{12}$; but as the Li projectiles are strongly absorbed and, furthermore, have energies close to the Coulomb barrier, it is hoped that these optical parameters generate distorted waves characteristic of Li^6 scattering from all the residual nuclei under consideration, at least as long as the corresponding Li^6 energies are near or below 7 MeV. The laboratory energies for Li^6 elastic scattering actually required for the calculations described range from 5.9 MeV for Be^9 to 15.3 MeV for N^{15} .

To obtain the form factor we have employed a more drastic assumption, which we call the quasifree alpha transfer or, in brief, "alpha transfer approximation." This approximation implies that the α cluster has the same structure in the target as in Li^6 , and that this structure is essentially that of a physical α particle (assumed to be fully space symmetric). We generate this "cluster wave function" as a solution for a mass-4 particle moving in a real Saxon (plus Coulomb) potential, i.e., we describe the four-nucleon cluster by a

TABLE I. Optical-model parameters for the deuteron and Li^6 distorted waves. (Best-fit Type A.)

Projectile	Target	V (MeV)	r_0 (F)	r_c (F)	a (F)	W' (MeV)	r_0' (F)	a' (F)	V_r (MeV)
d	C^{12}	117.1	0.900	1.3	0.982	56.0	1.800	0.405	(5.03)
d	C^{13}	114.9	0.900	1.3	0.964	50.3	1.800	0.393	(5.23)
d	O^{16}	107.5	0.884	1.3	0.915	26.2	1.593	0.684	(6.17)
d	O^{17}	85.3	1.100	1.3	0.902	35.9	1.600	0.509	(9.41)
d	O^{18}	86.3	1.105	1.3	0.939	39.7	1.608	0.598	(7.27)
d	F^{19}	92.2	0.965	1.3	0.888	35.8	1.461	0.813	(9.86)
Li^6	All	126.8	1.18	2.0	0.808	24.9	2.50	0.901	

³² W. W. Daehnick, L. J. Denes, D. Dittmer, and Y. S. Park (to be published).

³³ J. R. J. Bennett and I. S. Grant, in *Proceedings of the Third Conference on Reactions between Complex Nuclei, Asilomar, 1963*, edited by A. Ghiorso, R. M. Diamond, and H. E. Conzett (University of California Press, Berkeley, California, 1963).

²⁵ R. W. Ollerhead, C. Chasman, and D. A. Bromley, *Phys. Rev.* **134**, B74 (1964).

²⁶ P. H. Wackman and N. Austern, *Nucl. Phys.* **30**, 529 (1962); *Bull. Am. Phys. Soc.* **8**, 56 (1963).

²⁷ J. F. Gammel, B. J. Hill, and R. M. Thaler, *Phys. Rev.* **119**, 267 (1960).

²⁸ The assumed dominance of the d - α configuration in Li^6 is somewhat contrary to a strong He^3 - H^3 parentage for Li^6 suggested in the following reference: B. L. Berman, R. L. Bramblett, J. T. Caldwell, R. R. Harvey, and S. C. Fultz, *Phys. Rev. Letters* **15**, 727 (1965).

²⁹ R. M. Drisko, G. R. Satchler, and R. H. Bassel, in *Proceedings of the Third Conference on Reactions between Complex Nuclei, Asilomar, 1963*, edited by A. Ghiorso, R. M. Diamond, and H. E. Conzett (University of California Press, Berkeley, California, 1963), p. 85.

³⁰ R. H. Bassel, R. M. Drisko, and G. R. Satchler, Oak Ridge National Laboratory Report No. ORNL-3240, 1962 (unpublished).

³¹ N. Austern, R. M. Drisko, E. C. Halbert, and G. R. Satchler, *Phys. Rev.* **133**, B3 (1964).

“one-body” wave function, and formally treat the transfer of several nucleons like that of a single nucleon. The “cluster wave function” is restricted to the orbital angular momentum l needed for the reaction analyzed, and to a main quantum number N compatible with the simple shell-model (independent-particle model, I.P.M.) wave functions of the constituent nucleons.²⁹

In order to clarify this point we shall briefly describe, as a typical example, the $\text{O}^{17}(d, \text{Li}^6)\text{C}^{13}$ reaction. The lowest order shell-model ground state for the residual nucleus C^{13} (treating neutrons and protons alike) is

$$\{(\text{C}^{12})_0 + 1p_{1/2}\}_{1/2^-}.$$

For the target nucleus O^{17} we write

$$\{[(\text{C}^{12})_0 + 1p_{1/2}][1p_{1/2}^3]_{1/2} 1d_{5/2}\}_{5/2^+}.$$

Hence, if the four-nucleon pickup is to lead to the C^{13} ground state given above, the transferred nucleons must be those in the second bracket, i.e., one $1d$ nucleon and three $1p$ nucleons. If harmonic-oscillator wave functions are considered these 4 nucleons have a total of $3+2=5$ energy quanta. The Talmi transformation then demands that the internal plus external energy quanta of the cluster made up of these nucleons also total 5. If, furthermore, the four “cluster nucleons” are in a relative s state (as we assume in our “standard” calculations) there are no internal energy quanta, and the cluster must have 5 energy quanta associated with its center-of-mass motion. In shell-model language this means that the “cluster wave function” can only be $3p$, $2f$, or $1h$. Our alpha-transfer model allows us to further restrict the l value for the cluster wave function and the reaction as well. Let us now view $\text{O}^{17}_{5/2^+}$ as a two-body system [consisting of $\text{C}^{13}_{1/2^-}$ and α_{0^+}] in relative motion. Then one and only one relative orbital angular momentum (namely $l=3$) permits the system to be in the state $J^\pi = \frac{5}{2}^+$ which characterizes the O^{17} ground state. As alpha and deuteron are assumed to be in a relative s state (necessary for zero-range approximation) in the out-going projectile (Li^6), the l transfer according to this model must be 3. Therefore, in the first approximation the α cluster picked up from O^{17} should have a $2f$ center-of-mass motion.

It should probably be stressed that the harmonic oscillator and the independent-particle model so far are used only to uniquely fix cluster quantum numbers. However, they remain the basis for calculating four-nucleon parentages (as for instance for the target C^{12}) which will be compared with the “spectroscopic factors” obtained from (d, Li^6) experiments. The use of quasifree alpha form factors is not inconsistent with a shell-model picture of the nucleus, provided the implied residual interaction effects at large radii do not significantly modify the I.P.M. single-nucleon wave functions and the over-all probability of four-nucleon correlations. We do expect changes in the cluster wave functions for the extreme tail of the nuclear potential, for here the re-

sidual interactions are no longer negligible with respect to the average nuclear potential. As our reaction contributions mainly come from a region just outside the nucleus (Fig. 1) it seems realistic to calculate the form factor, loosely speaking, as a “bound cluster wave function” in a Saxon potential that yields an asymptotic form which takes some account of the residual interactions between the transferred nucleons.

The form-factor Saxon well is, strictly speaking, a calculational device, and its geometry cannot be measured. However, if our model is reasonable, the well dimensions should be related to those of corresponding scattering potentials. We have chosen the geometrical parameters on the basis of the following arguments: (a) Four-parameter optical-model analysis of α scattering from light nuclei yields complex well radii close to $R_{sc} = 2.0 \times A^{1/3}$ F, and diffusivities of 0.6 F.³⁴ Here R_{sc} is a number quite close to $R_{\text{O}^{16}} + R_{\alpha}$, and includes the finite size of the scattered particle. Such finite size compensation is probably desirable for our form-factor potential. (b) Optical-model radii are somewhat ambiguous since they are very sensitive to the depth of the scattering potentials chosen, but the Li^6 wave lengths are small compared to the known size of Li^6 ($R_{\text{Li}^6} \approx 2.8$ F), and it is possible to limit the range of physically meaningful form factor radii by semiclassical argu-

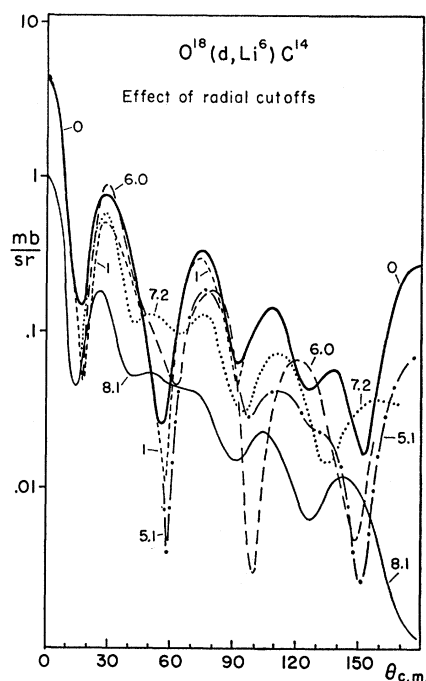


FIG. 1. Dependence of DWBA predictions for $\text{O}^{18}(d, \text{Li}^6)\text{C}^{14}$ on a lower radial integration cutoff. Cutoffs below 6F give results that are hardly distinguishable from 0 cutoff at forward angles. The important contributions to the reaction come from the region between 6 and 8 F.

³⁴ E. B. Carter, G. E. Mitchell, and H. R. Davis, Phys. Rev. 133, B1421 (1964).

ments. We would consider radii $r_0 A^{1/3}$ in the range $1.8 F < r_0 < 2.6 F$, with $1.2 F > a > 0.5 F$ as justifiable choices.

After exploring the effects of various form-factor radii for several reactions without finding drastic preferences we fixed, somewhat arbitrarily, $r_0 = 2.2 F$ and $a = 0.8 F$ for all calculations. For the individual reactions the depth of the form factor potential is adjusted to give a binding energy equal to the known α -particle separation energy. Figure 1 shows DWBA calculations for the reaction $O^{18}(d, Li^6)C^{14}$ as a function of a lower radial integration cutoff. It demonstrates that the main contributions to the reaction cross section come from radii between 6 and 8 F. We have *not* used radial cutoffs in the calculations later to be compared with experiment, mainly for two reasons: Sharp radial cutoffs although frequently employed are not realistic, and may give misleading results. Secondly, sharp cutoffs in the surface region can drastically affect the predicted cross sections and, hence, may be inadvertently used as fitting parameters. The latter point was considered particularly important here, since this study is not aimed at optimal fits, but rather at an open-minded investigation of the applicability of our interaction model.

The absolute normalization of our DWBA cross sections was estimated following Ref. 30. It may be in error by as much as an order of magnitude, but if we take our calculated cross sections at face value we find that they are of the same order of magnitude as the experimentally observed cross sections, apart from what might be called spectroscopic factors for "effective α clustering."

C. EXPERIMENTAL PROCEDURE

All (d, Li^6) reactions under investigation were initiated by roughly 15-MeV deuterons from the University of Pittsburgh's cyclotron. In addition to the previously investigated targets C^{12} , O^{16} , or F^{19} (Ref. 17), we prepared new, very thin targets containing C^{13} , O^{16} ,

O^{17} , O^{18} , or F^{19} in order to investigate (d, Li^6) cross sections in more of the light nuclei and recheck our previous results. The energy spectra for $M=6$ particles were separated from the other mass groups by two-parameter particle analysis consisting of simultaneous measurements of the time of flight and the energy of the particle. It has been shown previously by magnetic-rigidity-plus-energy analysis that the $M=6$ spectra consisted predominantly of Li^{6+++} ions.¹⁷ The particle detection systems have been described in detail in the same reference. Recently, several minor modifications have been incorporated into the time-of-flight system in order to improve its over-all performance, although the basic mode of operation remained identical to the original design. A schematic diagram of the current time-of-flight system is shown in Fig. 2. The modifications consist of a changed location for the T_0 (stop) detector, the use of a commercial time pickoff unit (Ortec Model 260), which utilizes the intrinsic fast rise time of the solid-state detector to obtain the event timing (start) signal, and the replacement of the E pulse amplifier by a Tennelec TC 200 amplifier. With these modifications, the over-all time-of-flight resolution for the various particle groups was typically between 2 and 3 nsec. An example of a time-of-flight spectrum of 6-MeV particles from O^{18} which traverse a 1-m flight path is shown in Fig. 3. In the time interval shown only masses 4, 6, 7, and 10 appear. The 3-nsec time resolution is seen to be adequate for separating the masses 6 and 7. For all particle groups which have been analyzed "cross talk" between adjacent mass groups has not been a significant problem. The time-of-flight setup was also used to investigate the energy dependence of the differential cross section. The deuteron beam was degraded by as much as 1.5 MeV in energy by the insertion of one of three different aluminum foils at the entrance aperture shown in Fig. 2. Intermediate absorber values were then obtained by rotating the absorber assembly. For each absorber setting the beam energy was measured by conventional magnetic analysis. The energy spread of the beam ranged from 80 keV at full energy (15 MeV) to about 200 keV at 13.5 MeV.

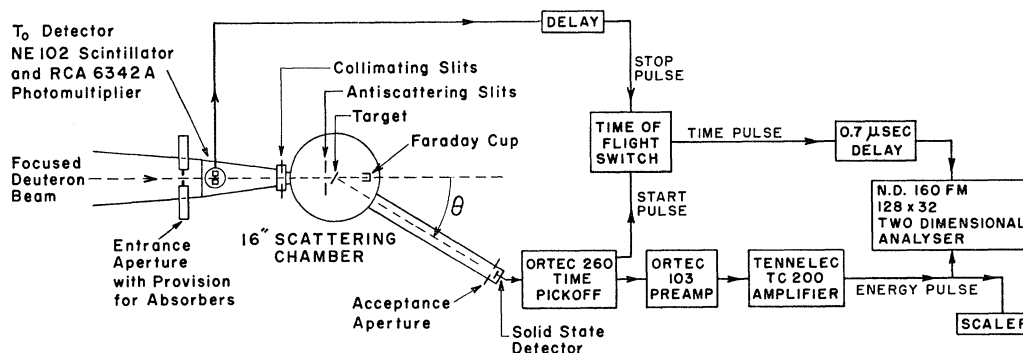


FIG. 2. Modified schematic for simultaneous time-of-flight and energy analysis. Experimental time-of-flight resolution varied between 2 and 3 nsec.

Targets

The O^{17} , O^{18} , and F^{19} targets were prepared by the deposition of thin layers of tungsten oxide (with oxygen enriched in O^{17} or O^{18}) or calcium fluoride on $100 \mu\text{g}/\text{cm}^2$ Ni backings. C^{13} targets were prepared by cracking methyl iodide (containing carbon enriched to 52% in C^{13}) on resistively heated $900\text{-}\mu\text{g}/\text{cm}^2$ Ni backings. Thicker foils were required in this case because the thin ones could not be handled in the manner required by this procedure. $900\text{-}\mu\text{g}/\text{cm}^2$ Ni foils were selected because Li^6 groups from the remote surface (as viewed by the detector) lost about 1 MeV in passing through the foil and were easily resolved from corresponding Li^6 groups from the near surface. All these targets were too thin and fragile to be weighed in order to find the target thickness. Instead, elastic scattering from O^{18} and F^{19} targets was compared with that from thicker O^{18} and F^{19} targets, which could be weighed. The thickness of the C^{13} and O^{17} targets could only be calculated by relying on the isotopic enrichment listed by the suppliers. The C^{13} targets used in this experiment had a C^{13} thickness of $8 \mu\text{g}/\text{cm}^2$, the two O^{17} enriched tungsten oxide targets had an O^{17} thickness of $52 \mu\text{g}/\text{cm}^2$ and $7 \mu\text{g}/\text{cm}^2$, respectively. The O^{18} enriched tungsten oxide target had an O^{18} target thickness of $36 \mu\text{g}/\text{cm}^2$, and the CaF_2 target had a F^{19} thickness of $84 \mu\text{g}/\text{cm}^2$.

Experimental Spectra

Examples of the energy spectra for mass-6 ions from C^{13} , O^{17} , O^{18} , and F^{19} targets are presented in Fig. 4. Contaminant Li^6 groups from C^{12} and to a lesser extent O^{16} are seen to be strong in all the spectra and a continuum of Li^6 ions from the 3-body breakup of the $(\text{C}^{12}+d)$ system dominates the low-energy regions. In Fig. 4(d), the $\text{C}^{13}(d, \text{Li}^6)\text{Be}^9$ peak stands out above the Li^6 continuum from the $(\text{C}^{12}+d)$ 3-body breakup, although the exact number of these ions is not very certain. This spectrum also exhibits a "ghost" spectrum approximately 1 MeV below the normal C^{12} or C^{13} spectrum. This is caused by the Li^6 ions originating at the far surface of the target which have been degraded in traversing the Ni "backing." The Li^6 ions from the $\text{O}^{17}(d, \text{Li}^6)\text{C}^{13}$ reaction [Fig. 4(c)] are just resolved from the Li^6 group from the $\text{O}^{18}(d, \text{Li}^6)\text{C}^{14}$ reaction. This target was extremely thin ($7 \mu\text{g}/\text{cm}^2$ of O^{17}), thus Li^6 ions from C^{12} and O^{16} contaminants are relatively abundant (note $\times 1/10$ scale). The $\text{O}^{18}(d, \text{Li}^6)\text{C}^{14}$ group from the O^{18} target [Fig. 4(b)] is well separated from all the other Li^6 groups since there was no appreciable O^{17} impurity in the O^{18} target. Similarly, Li^6 ions from the $\text{F}^{19}(d, \text{Li}^6)\text{N}^{15}$ ground-state reaction [Fig. 4(a)] are well resolved from all other Li^6 ions. This $M=6$ spectrum can be compared with a previous Li^6 spectrum from F^{19} obtained with a much thicker target.¹⁷ Li^6 ions leaving N^{15} in its first (or second) excited state near (5.28 MeV) seem as numerous as those which leave N^{15}

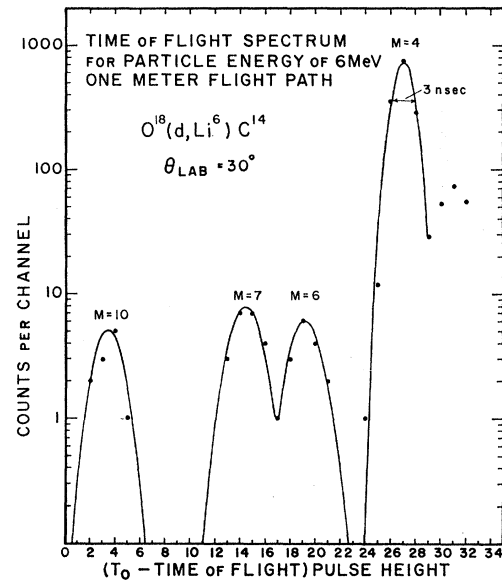


FIG. 3. Portion of a time-of-flight spectrum for particles having an energy of 6 MeV and a 1-m flight path. This target contained C^{12} , O^{16} , and O^{18} nuclei and was observed at $\theta_{\text{lab}}=30^\circ$. The time resolution is about 3 nsec.

in its ground state, even after subtraction of the background Li^6 ions from the $(\text{C}^{12}+d)$ 3-body breakup. There is a possibility that He^6 ions are present in the spectra from O^{18} and F^{19} [Figs. 4(a) and (b)]. A small $M=6$ group [Fig. 4(b)] superimposed on the continuum of Li^6 ions from the 3-body breakup of the $(\text{C}^{12}+d)$ system has been assigned tentatively as He^6 ions from the $\text{O}^{18}(d, \text{He}^6)\text{N}^{14}$ reaction, since this group is observed with the correct kinetic energy at this angle. In addition, similar groups are observed at neighboring angles with the appropriate kinematic shift in energy. The Li^6 background from C^{12} is too large to claim a similar effect in the case of any He^6 ions from the $\text{F}^{19}(d, \text{He}^6)\text{O}^{15}$ reaction. Magnetic analysis, which separates He^{6++} ions from Li^{6+++} ions, but not from Li^{6++} ions, did not show doubly charged, mass 6 ions at the He^6 energy for the ground-state transition significantly above what might be expected from background Li^{6++} ions [from the $\text{C}^{12}(d, \text{Li}^6)$ reaction] in either the O^{18} or F^{19} targets. The peak widths of the Li^6 groups are due primarily to the thickness of the target deposits on the foil backing. Straggling of Li^6 ions from the O^{17} and O^{18} targets is much more pronounced than in the C^{13} or F^{19} targets. This is attributed to straggling of the Li ions from the high- Z tungsten nuclei in the oxygen targets.

Errors

The experimental random errors due to statistics, background subtraction, particle group separation (time-of-flight and energy), and counting loss were estimated and combined. They are indicated by error

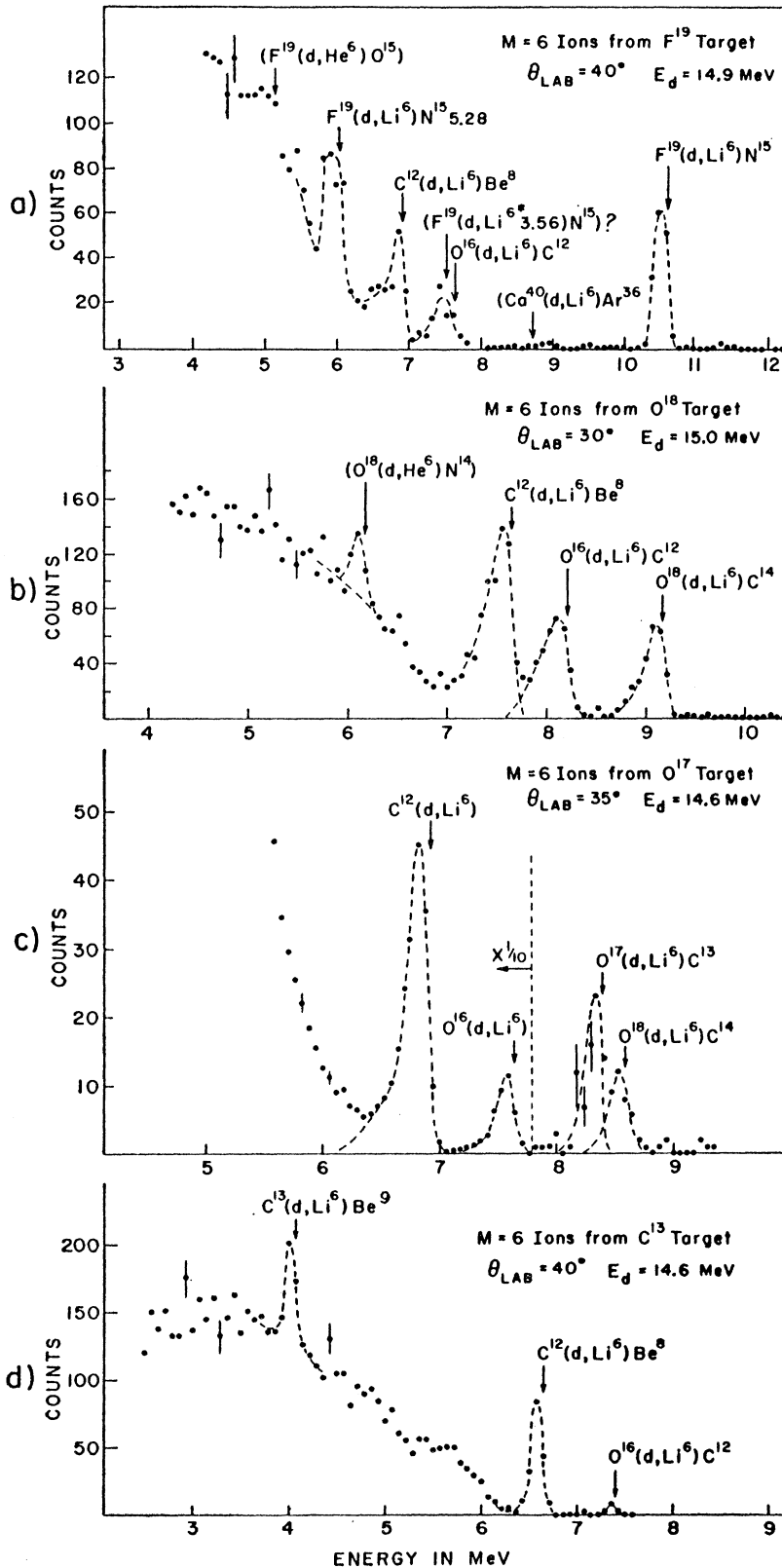


FIG. 4. Spectra of mass six particles from C^{13} , O^{17} , O^{18} , and F^{19} targets as obtained from energy-time-of-flight analysis. Dashed lines mark the ground-state groups of interest. Peak widths are due to target thickness, not detector resolution. The arrows for reactions in parentheses are placed at the expected energy position for the ions and do not necessarily assert their presence.

bars for each differential cross-section point. Contaminants in the targets were not a significant source of error for the measured reactions. The high- Z elements in the targets (i.e., Ni, Ca, or W) do not produce any detectable heavy fragment background. After prolonged use of the targets it was found that there was an appreciable buildup of C^{12} and O^{16} contaminations. Fortunately, the main interest for the O^{17} , O^{18} , and F^{19} targets was in particle groups with kinetic energies greater than those of the groups from C^{12} and O^{16} . However, subtraction of the Li^6 ions due to the $(C^{12}+d)$ 3-body breakup was necessary in the case of the C^{13} target, in order to extract the Li^6 cross sections for the $C^{13}(d, Li^6)Be^9$ ground-state reaction. This led to quite large uncertainties in the cross-section measurements for the $C^{13}(d, Li^6)Be^9$ reaction.

A lower limit to the systematic errors which are associated with the absolute cross sections given has been obtained from deuteron elastic scattering on these and other target nuclei. It has been concluded from the reproducibility of the elastic scattering and from a comparison of low-angle platinum elastic scattering to Coulomb scattering, that the scale error in experiments using our scattering facilities is usually only $\pm 10\%$,

provided good uniform targets are used. The average target thickness, measured by a comparison of its elastic scattering with thicker, known composition targets could be determined to 10%. However many of the targets were not uniform and the reproducibility of absolute (d, Li^6) cross sections with thin targets does not appear to be better than 20%. Therefore we assign an over-all uncertainty of $\pm 20\%$ to the absolute cross-section scale.

The energy of the incident beam was measured accurately for each angular distribution and the deuteron energy was kept constant for each particular angular distribution. The energy spread of the beam was about 80 keV and, allowing for a ± 20 -keV drift in the median energy, a ± 50 keV uncertainty is assigned to the measured average deuteron energy.

D. EXPERIMENTAL RESULTS

The center-of-mass angular distributions for (d, Li^6) reactions from C^{12} , C^{13} , O^{16} , O^{17} , O^{18} , and F^{19} are shown in Fig. 5. The cluster pickup model allows only one l transfer in each of these reactions. The angular distributions for the $l=0$ transfers in C^{12} , O^{16} , and O^{18} along

FIG. 5. Differential cross sections (c.m.) for (d, Li^6) reactions in light nuclei. The error bars contain all random experimental errors. Solid lines represent our DWBA predictions for these reactions. The dashed line in Fig. 5(b) represents the results of a finite-range calculation.

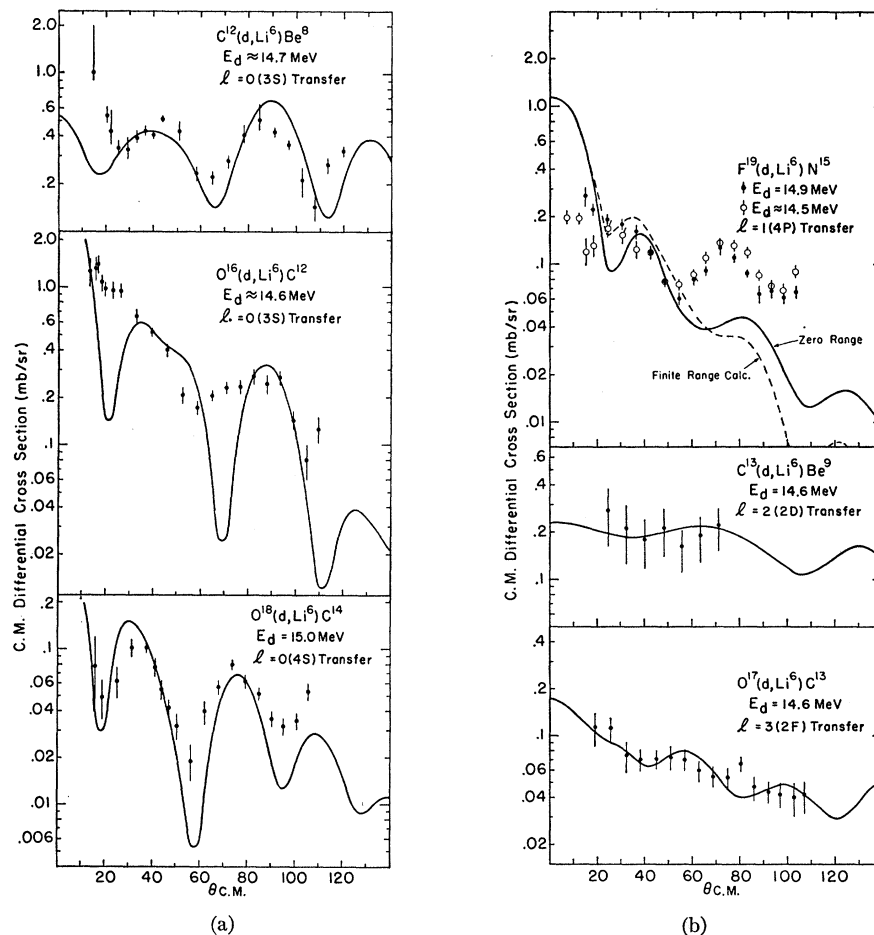


TABLE II. Total cross sections for (d, Li^6) reactions.

Target	Approximate barrier penetrability	σ_T (mb) best est.	$\sigma_T(\text{expt})/\sigma_T(\text{DWBA})$	$S_\alpha/S_\alpha(C^{12})$
C^{12}	0.90	4.2	0.60	1.0
C^{13}	0.50	2.0	1.20	2.0
O^{16}	0.80	2.9	3.00	5.0
O^{17}	0.85	0.65	0.30	0.50
O^{18}	0.85	0.60	0.20	0.34
F^{19}	0.90	1.4	(0.30)	(0.50)

with the two distributions for the $l=1$ transfer in F^{19} taken at different energies have quite similar characteristics. They are forward-peaked and have strong oscillatory behavior, resembling diffraction patterns characteristic of direct surface reactions. The positions of the maxima are regularly spaced, and they move together and to smaller angles with increasing mass number. A weak diffractive character can still be seen in the $l=3$ transfer from O^{17} although now the minima appear to be "washed out." If a simple pickup mechanism applies, then the strong diffractive effects diminish with increasing l transfer in the manner shown by the DWBA predictions (solid lines in Fig. 5) and the diffractive pattern shifts toward larger angles. These characteristics are quite similar to those observed in single-nucleon transfers such as (d, p) stripping or (d, t) pickup reactions.

Total cross sections for these (d, Li^6) reactions were estimated and are listed in Table II. The cross sections are quite large, of the order of 1 mb, although they do vary by a factor of 5 over this mass region. The Li^6 energies are near the Coulomb barrier, hence the cross sections decrease rapidly with increasing charge number of the target. Indeed, for Al^{27} heavy-ion fragments could not be observed above the background.

Effect of Energy Variations on the Angular Distributions

A comparison of the two angular distributions taken at 14.5 and 14.9 MeV for F^{19} (Fig. 5) shows that at the lower energy, the first minimum is more pronounced, but otherwise the angular distributions have similar magnitudes and gross structure. Since one important criterion for a direct reaction is that its cross section vary smoothly with incident bombarding energy, the two angular distributions for F^{19} suggest that while compound effects are present, they are not particularly pronounced at these bombarding energies. Further insight into the nature of the reaction mechanism was obtained by investigating the detailed dependence of the differential cross sections for C^{12} with incident bombarding energy. C^{12} was the lightest target and most suspect to give compound contributions. $C^{12}(d, Li^6)$ excitation functions were taken at the first minimum $\theta_{lab}=18^\circ$ and the first maximum $\theta_{lab}=30^\circ$. The results are shown in Fig. 6. The excitation function at 18° shows

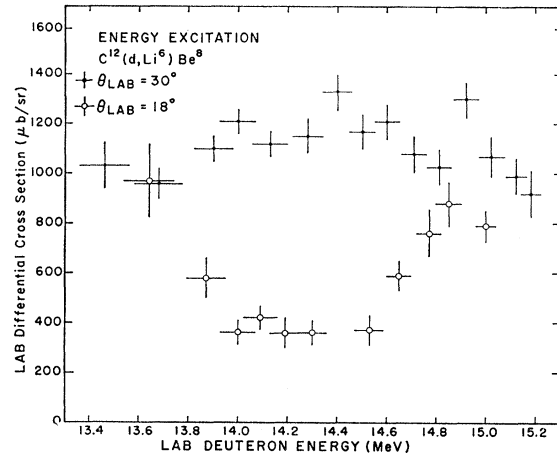


FIG. 6. Excitation functions for $C^{12}(d, Li^6)Be^8$. The closed circles represent data near the 30° diffraction maximum. Open circles represent the cross section at $\theta_{lab}=18^\circ$, near the first diffraction minimum.

a slow but pronounced energy dependence, while the excitation function at 30° shows no pronounced energy dependence and appears uncorrelated with the energy dependence at the 18° minimum. It is obvious that energy variations influence the detailed shape of the angular distributions, particularly, as might be expected at the minima of the diffraction patterns. For O^{16} the measurements of elastic deuteron scattering indicates noticeable cross-section fluctuations with energy near $E_d=15$ MeV. In $C^{12}(d, Li^6)$ and $F^{19}(d, Li^6)$ fluctuations are only seen near the first DWBA minimum. It is possible that these energy-dependent effects are due to high-spin resonances in the exit channels, similar to those in α scattering.³⁵ High-spin resonances would be most visible at very small and very large angles. We would not say that these energy-dependent effects are insignificant, but we feel that they are not drastic enough to shake one's belief that the reactions may primarily be described as direct transfer reactions. They do indicate that one should not expect perfect agreement of simple direct-interaction theory (i.e., DWBA) and the experimental angular distributions at these energies.

E. DISCUSSION

The comparison of data and DWBA predictions in Fig. 5 shows strikingly similar characteristics and generally good agreement. This is particularly significant in view of the fact that no fitting parameters were used and all distorted waves result from the best available elastic-scattering data. Quantitative disagreements generally are found at the DWBA minima which for $\Delta l=0$ are always too deep. Here compound contributions to the reaction can be expected to be most visible. It is hard to assess which of the disagreements are brought on by the lack of complete Li scattering data,

³⁵ D. Robson (private communication).

but it is likely that those effects will be most drastic for $\text{F}^{19}(d, \text{Li}^6)$, where the equivalent Li^6 laboratory energy is 15 MeV, 8 MeV higher than in the $\text{C}^{12}(\text{Li}^7, \text{Li}^7)$ experiment that determined the Li potentials used. Indeed, in the case of $\text{F}^{19}(d, \text{Li}^6)\text{N}^{15}$ there is little resemblance between the experimental data and the DWBA $\Delta l=1$ prediction. The general slope of the theoretical curve is much too steep and the oscillations are about 90° out of phase. The situation is not improved by taking finite range into account accurately [dotted curve in Fig. 5(d)]. In fact, the finite-range prediction looks qualitatively much like the zero-range curve, and falls off even faster.

In analogy to customary pickup and stripping work our numerical calculations were made with the assumption that the target contains exactly one cluster, the transfer of which would leave the residual nucleus in the observed final state. Furthermore, we assumed for the calculation that Li^6 has a parentage of exactly one deuteron and one " α " cluster. Both assumptions, of course, are only made for normalization purposes so that our final calculational result must contain two factors S_α and $S_{\alpha d}$, which in case that our model is fully applicable might be called "cluster spectroscopic factors" for the target nucleus and the outgoing projectile, respectively. For properly normalized DWBA predictions the ratio of experimental cross section over calculated cross section $\sigma_{\text{expt}}/\sigma_{\text{DWBA}}$ thus should equal the product $S_\alpha S_{\alpha d}$.

As mentioned in Sec. B the absolute normalization of our DWBA calculations is only certain to about an order of magnitude. This, however, does not prevent us from using the (d, Li^6) calculations for spectroscopic purposes if we decide that our model is adequate. The unknown normalization correction η is the same for all calculations, so is the factor $S_{\alpha d}$, hence once we know S_α for one of the six targets we can determine $\eta S_{\alpha d}$, and the values S_α for the other ones can be obtained also. A calculation of S_α for C^{12} was made, using the prescription by Smirnov³⁶ and independent-particle model wave functions for C^{12} . A value very close to one was found.¹⁵ $S_\alpha(\text{C}^{12})=1$ leads to $\eta S_{\alpha d}=0.6$, a number which suggests that η is surprisingly close to one.

Column 5 in Table II lists the values of S_α based on $S_\alpha(\text{C}^{12})=1$, and shows an interesting trend. As long as all transferred nucleons are $1p$ nucleons (in C^{12} , C^{13} , O^{16}) S_α increases rapidly with the number of available $1p$ nucleons. However, as soon as the ground transition requires that nucleons from the $2s$, $1d$ as well as the $1p$ shell must be transferred (in O^{17} , O^{18} , and F^{19}) S_α decreases by almost an order of magnitude. This trend agrees very well with an independent-particle picture of the nucleus. It would be most interesting to see if similar S_α ratios will be obtained for (d, Li^6) reactions at higher energies.

³⁶ Yu. F. Smirnov and D. Chlebowska, Nucl. Phys. **26**, 306 (1961).

In a search for possible modifications of DWBA calculations which might lead to improved agreement while remaining within the framework of our alpha-cluster pickup model, several variations have been performed on the standard DWBA calculations. These variations are of four general types:

(1) Evaluation of the effects of reasonable variations in the geometrical parameters for the Saxon potential used to generate the form factor.

(2) DWBA calculations with distorted deuteron waves generated from optical-model potentials which were obtained without the use of an $\mathbf{l} \cdot \mathbf{s}$ term (Type B).²⁰

(3) Evaluation of the effects of higher shell-model configuration admixtures to the ground-state wave functions.

(4) Use of angular-momentum transfers which are not predicted by the simplest cluster transfer model. Such l values occur in the transfer of an excited 2^+ cluster, where $l_\alpha^* = l \pm 2$.

(Kurath's³⁷ calculation of the quadrupole deformation of Li^7 has shown that the excited alpha-core component in Li^7 is not small.) Examples of predictions resulting from these variations of the standard (no free parameter) DWBA calculations are shown in Fig. 7. The solid curve for the $\text{O}^{18}(d, \text{Li}^6)\text{C}^{14}$ reaction shows a calculation with the same parameters as the O^{18} prediction in Fig. 5 with the exception that the form-factor diffuseness parameter a has been decreased from 0.8 to 0.6 F. This variation leads to a qualitatively better agreement with the data for O^{18} . It was observed more generally that minor adjustments of the diffuseness parameter a will usually improve agreement. It should be noted that the calculations are really sensitive to $(R+a)$. Once a suitable radius R is chosen only a variation in the diffuseness parameter a need be considered or vice versa. The dashed curve in Fig. 7(a) is calculated under the same conditions as the solid curve except that a Type-B deuteron optical potential²⁰ is used to generate the distorted deuteron waves. For this example the agreement is certainly inferior to the Type A, $V_s=0$ potential (Table I). However, the calculations do not always indicate a preference of one type of optical potential over the other.

Admixtures of higher shell-model configurations to the ground-state wave functions are not well known, hence calculations including these admixtures have not been made. In the DWBA calculations, consideration of higher target configurations attributes to the transferred cluster higher values of N , the principal quantum number of its center-of-mass motion. The contributions of various allowed values of N are coherent, so it would not be proper to simply add cross sections. Instead the form factor integral $F(r)$ should be replaced by $\sum_N a_N F_N(r)$, where a_N is the coefficient giving the strength of the configuration. Some DWBA calculations

³⁷ D. Kurath, Phys. Rev. **140**, B1190 (1965).

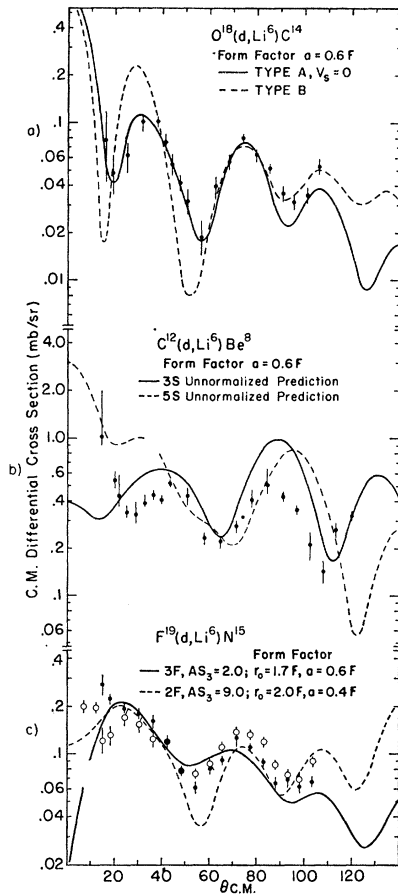


FIG. 7. Examples of the effect of parameter changes on DWBA calculations. The solid curve in 7(a) and the curves in 7(c) are not referred to as predictions, because arbitrary (though minor) changes in the form factor were made in order to improve agreement with experiment.

have been done by replacing the lowest predicted N by a value N' corresponding to higher configurations. An example of this type of calculation is shown for the $N=5$ case in C^{12} as the dashed curve in Fig. 7(b). The corresponding (standard) $N=3$ calculation is shown by the solid curve for comparison. It is seen that the $N=5$ calculation does predict a strong forward peaking in C^{12} not predicted in the $N=3$ case. Forward peaking and shifting of the diffraction pattern to higher angles for higher N are also observed in calculations for other targets, and often the agreement becomes superior to the lower N calculations. Such improvements, however, do not necessarily mean that higher configurations are very important. It is known that zero-range, local potential DWBA calculations overestimate the contribution from the nuclear interior, and as the form factors for higher N have more nodes in the nuclear interior, contributions to the scattering amplitude from this region are more likely to average to zero than for the form factors with smaller N .

DWBA reactions calculated by simply replacing the

transferred angular momentum l by $l \pm 2$ usually predict angular distributions which are about 180° out of phase with the predictions for the value l . Since the experimental (d, Li^6) angular distributions in most cases are correctly given by the simplest l transfer, the $l \pm 2$ calculations give poor agreement. This is true for all (d, Li^6) reactions, except for F^{19} where our standard predictions are out of phase with the data. In this case one can fit phase and periodicity of $\sigma(\theta)_{\text{expt}}$ with an $l=3$ transition, but the general slope of these predictions remains in disagreement unless simultaneous changes in the geometrical parameters r_0 and a of the form-factor potential are made. Hence, the calculations shown in Fig. 7(c) are merely fits and not in the spirit of our other DWBA calculations.

F. SUMMARY AND CONCLUSIONS

The experimental (d, Li^6) cross sections for all targets investigated have the diffractive nature and absolute magnitudes suggestive of single-step surface reactions. The minor sensitivity of the differential cross sections to changes in the incident deuteron energy indicates that energy-dependent effects in these reactions may no longer be important at 15 MeV. (d, Li^6) reactions investigated at other energies ($E_d < 13.5$ MeV,¹⁶ $E_d \approx 12-13$ MeV,²¹ $E_d \approx 21$ MeV,¹⁹ and $E_d = 34.2$ MeV²²) on corresponding targets show similar characteristics in their angular distributions, in support of a direct transfer interpretation. This must be contrasted with the $O^{16}(\alpha, Be^8)C^{12}$ reaction which even at energies of 35.5 to 41.9 MeV shows very strong fluctuations in the differential cross sections.²⁴

For (d, Li^6) reactions near 15 MeV the current DWBA predictions for four-nucleon cluster transfers (Fig. 5) seem to be in acceptable agreement with the experimental angular distributions. The gross structure and the magnitude of the cross sections are correctly predicted for all cases with the exception of the $F^{19}(d, Li^6)N^{15}$ reaction. This is remarkable in view of all the simplifying approximations imposed on this transfer model.

There are some obvious deficiencies in the present calculations that may be removable in the near future. Firstly, a better form factor may be obtainable from microscopic independent-particle model calculations. Such calculations have been started. Secondly, Li^6 elastic-scattering data from the residual targets at appropriate energies should become available for optical-model analysis and make possible the use of more realistic distorted Li^6 waves. Thirdly, a better representation of the wave functions in the nuclear interior should be possible.³⁸ The optical potentials used in generating the distorted waves are local potentials, and the effects of nonlocality are usually treated by introducing energy-dependent parameters. However, nonlocality

³⁸ G. R. Satchler (private communication).

reduces the projectile wave functions in the nuclear interior compared to those for "equivalent" local potentials. A simple nonlocality correction factor may be applied to the wave function generated by the local potentials.³⁹ In the cluster transfer calculations a similar radial correction factor may routinely be used in zero-range calculations to compensate for finite range effects,^{39,40} instead of the more time-consuming exact finite range calculation³¹ that we made for a few cases. If the inclusion of these improvements and refinements in (d, Li^6) calculations should lead to even better agreement with experiment one ought to feel quite confident that the single-step cluster transfer model is sufficiently realistic to be used in the analysis of (d, Li^6) data. We realize that our present calculations do not even exhaust

all effects that direct interaction theory in general recognizes as important. In particular, recoil and exchange terms may be quite important for our light targets. Nevertheless, it is felt that the present simple reaction model has been surprisingly successful, and may be even more useful for higher energies and heavier targets.

Keeping in mind our qualified acceptance of the proposed (d, Li^6) reaction mechanism we again refer to the spectroscopic information contained in Table II. There is no doubt that a drastic difference exists for α pickup from p shell and the light s, d shell nuclei. The deducible α parentages for the target ground states agree, at least qualitatively, with simple shell-model expectations.^{36,11} The dominance of simple shell-model configurations is also indicated by the quite comparable probability for 5-nucleon transfer reactions observed in the s, d shell nuclei.^{23,41}

³⁹ J. K. Dickens and F. G. Perey, Oak Ridge National Laboratory Report No. ORNL-3858, 1965 (unpublished).

⁴⁰ J. K. Dickens, R. M. Drisko, F. G. Perey, and G. R. Satchler, Phys. Letters 15, 337 (1965).

⁴¹ L. J. Denes and W. W. Daehnick (to be published).

Elastic and Inelastic Electron Scattering from C^{12} and O^{16} †

HALL CRANNELL

High Energy Physics Laboratory, Stanford University, Stanford, California

(Received 3 March 1966)

Elastic and inelastic electron scattering from C^{12} and O^{16} has been studied for various scattered electron angles, using primary beam energies from 600 to 800 MeV. These studies cover a range of the square of the momentum transferred to the nucleus of 2.79 to 11.45 F^{-2} for C^{12} , and 2.79 to 8.52 F^{-2} for O^{16} . A procedure for subtracting the effects of energy loss due to radiation of the electrons is developed. With the resolution obtained in this experiment it is possible to resolve elastically scattered electrons from inelastically scattered electrons. In many instances it is also possible to resolve electrons which have excited discrete nuclear levels in C^{12} and O^{16} . Inelastic electron scattering due to excitation of nuclear levels is observed for the 4.43-MeV 2^+ and 9.6-MeV 3^- levels in C^{12} , and for the 6.1-MeV levels in O^{16} . Differential cross sections for excitation of these levels as well as for elastic scattering are determined. Absolute values of the cross sections are obtained by comparison with known absolute proton cross sections. Analysis of the data using the first Born approximation shows that the root-mean-square radii of C^{12} and O^{16} are $2.40 \pm 0.02 F$ and $2.65 \pm 0.04 F$, respectively.

I. INTRODUCTION

THE advent of high-energy electron accelerators has facilitated experimentation aimed at gaining more detailed knowledge about the electromagnetic charge distributions of nuclei. These experiments have consisted of scattering high-energy electrons from target nuclei and studying the energy and angular distribution of the scattered electrons.¹ This investigation² involved a study of elastic and inelastic electron scattering from two nuclei, C^{12} and O^{16} . Both of these nuclei have

already been the subject of investigation by several experimenters.³⁻⁶ Because these nuclei have been studied so extensively in the past, it is interesting to consider the factors that motivated additional experimental work at this time.

The most sensitive region of electron-scattering measurements of nuclear characteristics is near a diffraction minimum in the cross section. The most successful model to date for P -shell nuclei, the harmonic-well shell model, predicts only one diffraction minimum

† Work supported in part by the U. S. Office of Naval Research, Contract [Nonr 225(67)].

¹ A general review has been given by R. Hofstadter, Ann. Rev. Nucl. Sci. 7, 231 (1957).

² A more detailed description of this experiment is given in the author's Ph.D. thesis, Stanford University, 1964 (unpublished).

³ J. H. Fregeau, Ph.D. thesis, Stanford University, 1956 (unpublished).

⁴ J. H. Fregeau and R. Hofstadter, Phys. Rev. 99, 1503 (1955).

⁵ H. F. Ehrenberg, R. Hofstadter, U. Meyer-Berkhout, D. G. Ravenhall, and S. E. Sobottka, Phys. Rev. 113, 666 (1959).

⁶ U. Meyer-Berkhout, K. W. Ford, and A. E. S. Green, Ann. Phys. 8 (N. Y.), 119 (1959).